



A Highly Attenuated Vesicular Stomatitis Virus-Based Vaccine Platform Controls Hepatitis B Virus Replication in Mouse Models of Hepatitis B

Safiekhatoon Moshkani,^a Carolina Chiale,^a Sabine M. Lang,^b John K. Rose,^b Michael D. Robek^a

^aDepartment of Immunology and Microbial Disease, Albany Medical College, Albany, New York, USA

^bDepartment of Pathology, Yale School of Medicine, New Haven, Connecticut, USA

ABSTRACT Therapeutic vaccines may be an important component of a treatment regimen for curing chronic hepatitis B virus (HBV) infection. We previously demonstrated that recombinant wild-type vesicular stomatitis virus (VSV) expressing the HBV middle surface glycoprotein (MHBs) elicits functional immune responses in mouse models of HBV replication. However, VSV has some undesirable pathogenic properties, and the use of this platform in humans requires further viral attenuation. We therefore generated a highly attenuated VSV that expresses MHBs and contains two attenuating mutations. This vector was evaluated for immunogenicity, pathogenesis, and anti-HBV function in mice. Compared to wild-type VSV, the highly attenuated virus displayed markedly reduced pathogenesis but induced similar MHBs-specific CD8⁺ T cell and antibody responses. The CD8⁺ T cell responses elicited by this vector in naive mice prevented HBV replication in animals that were later challenged by hydrodynamic injection or transduction with adeno-associated virus encoding the HBV genome (AAV-HBV). In mice in which persistent HBV replication was first established by AAV-HBV transduction, subsequent immunization with the attenuated VSV induced MHBs-specific CD8⁺ T cell responses that corresponded with reductions in serum and liver HBV antigens and nucleic acids. HBV control was associated with an increase in the frequency of intrahepatic HBV-specific CD8⁺ T cells and a transient elevation in serum alanine aminotransferase activity. The ability of VSV to induce a robust multispecific T cell response that controls HBV replication combined with the improved safety profile of the highly attenuated vector suggests that this platform offers a new approach for HBV therapeutic vaccination.

IMPORTANCE A curative treatment for chronic hepatitis B must eliminate the virus from the liver, but current antiviral therapies typically fail to do so. Immune-mediated resolution of infection occurs in a small fraction of chronic HBV patients, which suggests the potential efficacy of therapeutic strategies that boost the patient's own immune response to the virus. We modified a safe form of VSV to express an immunogenic HBV protein and evaluated the efficacy of this vector in the prevention and treatment of HBV infection in mouse models. Our results show that this vector elicits HBV-specific immune responses that prevent the establishment of HBV infection and reduce viral proteins in the serum and viral DNA/RNA in the liver of mice with persistent HBV replication. These findings suggest that highly attenuated and safe virus-based vaccine platforms have the potential to be utilized for the development of an effective therapeutic vaccine against chronic HBV infection.

KEYWORDS adeno-associated virus, chronic hepatitis B, immunotherapy, immunotolerance, therapeutic vaccines, vesicular stomatitis virus

Citation Moshkani S, Chiale C, Lang SM, Rose JK, Robek MD. 2019. A highly attenuated vesicular stomatitis virus-based vaccine platform controls hepatitis B virus replication in mouse models of hepatitis B. *J Virol* 93:e01586-18. <https://doi.org/10.1128/JVI.01586-18>.

Editor J.-H. James Ou, University of Southern California

Copyright © 2019 American Society for Microbiology. All Rights Reserved.

Address correspondence to Michael D. Robek, robekm@amc.edu.

Received 9 September 2018

Accepted 7 December 2018

Accepted manuscript posted online 12 December 2018

Published 19 February 2019

Despite the availability of an effective preventative vaccine, chronic hepatitis B virus (HBV) infection affects over 250 million people worldwide and causes a significant number of deaths each year due to complications such as liver cirrhosis and hepatocellular carcinoma (1). Current nucleos(t)ide-based antiviral therapies are effective at reducing viremia but are not able to eliminate the HBV covalently closed circular DNA minichromosome that persists in the nuclei of infected hepatocytes and serves as a template for new virion production (2). Lifelong antiviral treatment is also costly and is associated with possible adverse side effects and the risk of developing viral resistance.

Acute HBV infection during adulthood typically generates a relatively strong and multispecific T cell response that leads to effective virus control. On the contrary, HBV infection in early childhood leads to lifelong persistence of the infection, and the majority of antigen (Ag)-specific T cells in these patients display impaired functions or exhausted phenotypes or are deleted (3). Spontaneous chronic HBV resolution in some patients (4) and viral clearance after acute HBV infection suggest that immune-based strategies that aim to augment adaptive immunity might be an effective approach for the treatment of chronic hepatitis B (5). A successful therapeutic strategy must be able to generate potent and durable T cell-mediated immunity to control HBV replication and to eliminate HBV-infected hepatocytes. While the current HBV vaccine induces protective antibodies (Abs) that prevent infection, it does not elicit the virus-specific CD8⁺ T cells needed to control an established infection. A number of protein-, DNA-, and virus-based vaccine regimens have shown promising efficacy in preclinical mouse and woodchuck models of persistent hepadnavirus infection (reviewed in reference 6). Although recombinant protein- and DNA-based vaccines have failed to generate an effective therapeutic response in humans (7), alternative immunotherapeutic strategies, such as blocking T cell-inhibitory signals, engineering HBV-specific T cells, or employing more highly immunogenic vaccine platforms, have been proposed (8). Replicating virus-based vectors that stimulate the immune system through their adjuvant effects and induce strong CD8⁺ T cell responses might be a beneficial tool for the development of a therapeutic vaccine against chronic HBV infection.

Due to favorable features, including its low seroprevalence, simplicity, and robust foreign antigen expression, recombinant vesicular stomatitis virus (VSV) has been used for the development of vaccines against a variety of human pathogens, and these vaccines have shown potential efficacy in nonhuman primates (9) and humans (10). Previously, we analyzed the immunogenicity and function of recombinant wild-type VSV expressing the HBV middle surface glycoprotein (MHBs). We found that the CD8⁺ T cell responses elicited by VSV-MHBs were superior to those generated by a single dose of other vaccine platforms, including recombinant protein and vaccinia virus; were protective in a mouse model of acute HBV replication; and could be induced in tolerant HBV transgenic (HBV^{tg}) mice (11, 12).

Due to safety concerns regarding the use of wild-type VSV in humans, a highly attenuated virus with significantly reduced neurovirulence in mice (13) was further modified to express foreign antigens from the first genome position by Cooper et al. (14). This vector (N4CT1) contains the nucleocapsid (N) gene translocated from the first genome position to the fourth (N4) and a glycoprotein (G) cytoplasmic tail truncation to a single amino acid (CT1). Modified N4CT1 vectors expressing different viral proteins have been validated as safe and immunogenic in nonhuman primates (15–17), and the platform was also recently shown to be immunogenic and well tolerated in a human HIV vaccine clinical trial (18, 19).

These studies therefore led us to utilize the N4CT1 platform for MHBs expression and to investigate the preventative and therapeutic potential of this vector in a recently described mouse model of persistent HBV replication based on adeno-associated virus (AAV)-mediated transduction of HBV genomes into the liver (20). Here, we found that N4CT1-MHBs generates immune responses that both prevent and control persistent HBV infection in mice. The safety profile, immunogenicity, and the ability of N4CT1-MHBs to control virus replication and overcome immune dysfunction in a mouse model of persistent HBV infection suggest that highly attenuated VSV-based vaccine platforms

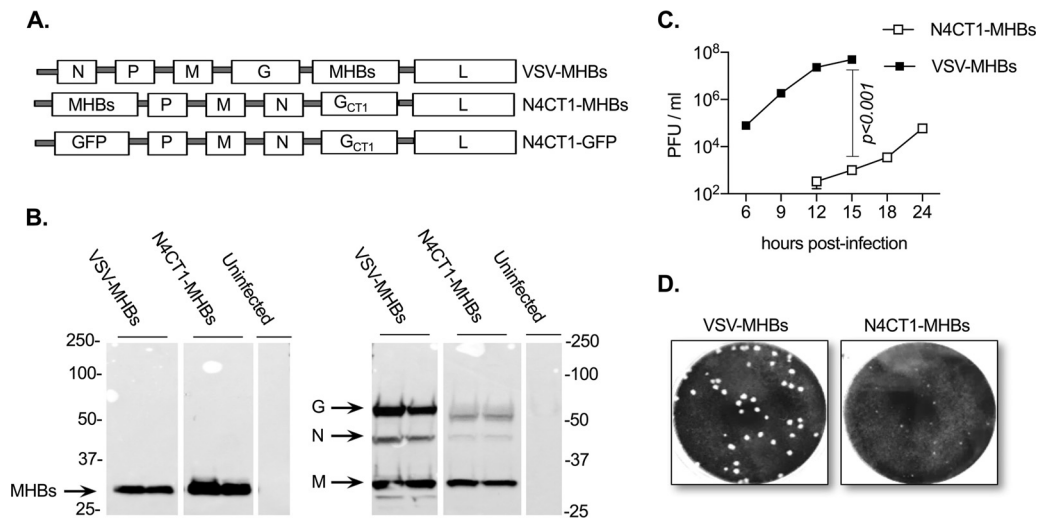


FIG 1 Compared to VSV-MHBs, N4CT1-MHBs displays a low replication rate and reduced cytopathic effects *in vitro*. (A) VSV vectors used for immunizations. (B) BHK cells were infected with the indicated viruses or not infected, and cell lysates were collected at 12 h postinfection and assayed for MHBs or VSV protein (M, N, and G) expression by Western blotting. (C) BHK cells in triplicate wells were infected with the indicated viruses, and the titers in medium were determined to compare the replication of both viruses. Error bars denote standard errors of the means (SEM). (D) Plaque size comparison in infected BHK cells.

may offer a new strategy for the development of an HBV vaccine with both preventative and therapeutic potential.

RESULTS

N4CT1-MHBs displays a low replication rate and reduced cytopathic effects *in vitro* compared to VSV-MHBs. For comparison to N4CT1-MHBs, we used nonattenuated VSV expressing MHBs from the fifth genome position (VSV-MHBs) as a positive control (11) and N4CT1 expressing green fluorescent protein (GFP) (N4CT1-GFP) as a negative control (Fig. 1A). MHBs expression in infected BHK cells was confirmed by Western blot analysis (Fig. 1B). The higher MHBs expression level in N4CT1-MHBs-infected cells than in VSV-MHBs-infected cells is likely due to the difference in the MHBs position in the VSV genomes (Fig. 1A), as first-genome-position vectors have higher foreign protein expression levels than fifth-position vectors (16, 17). The low VSV nucleocapsid protein (N) and glycoprotein (G) expression levels relative to matrix (M) in cells infected with N4CT1-MHBs are consistent with the presence of the attenuating mutations (Fig. 1B). As expected, compared to VSV-MHBs, N4CT1-MHBs showed a significantly low replication rate in BHK cells (Fig. 1C) and generated small plaques (Fig. 1D), thus confirming the generation of attenuated virus.

N4CT1-MHBs immunization of naive mice generates immune responses similar to those immunized with VSV-MHBs. Pathological effects and immunogenicity of N4CT1-MHBs were next evaluated in mice. Intranasal (i.n.) N4CT1-MHBs administration showed markedly reduced pathogenesis compared to VSV-MHBs, as measured by weight loss (Fig. 2A). In addition to maintaining normal weight, the N4CT1-MHBs-infected mice also did not show any other overt signs of distress. The ability of N4CT1-MHBs to elicit Ag-specific CD8⁺ T cell responses was investigated by intramuscular (i.m.) immunization of naive CB6F1 mice with N4CT1-MHBs or VSV-MHBs. CD8⁺ T cell response analysis on day 7 postimmunization showed that similar to VSV-MHBs, immunization with N4CT1-MHBs elicited Ag-specific CD8⁺ T cells against all four MHBs epitopes (Fig. 2B). The ability of N4CT1-MHBs to induce Ag-specific Ab responses was evaluated by an enzyme-linked immunosorbent assay (ELISA) using serum samples collected on week 8 postimmunization. HBs-specific antibody was detected in the majority of the mice that received either VSV-MHBs or N4CT1-MHBs (Fig. 2C). To further evaluate N4CT1-MHBs immunogenicity in a highly diverse genetic background, we

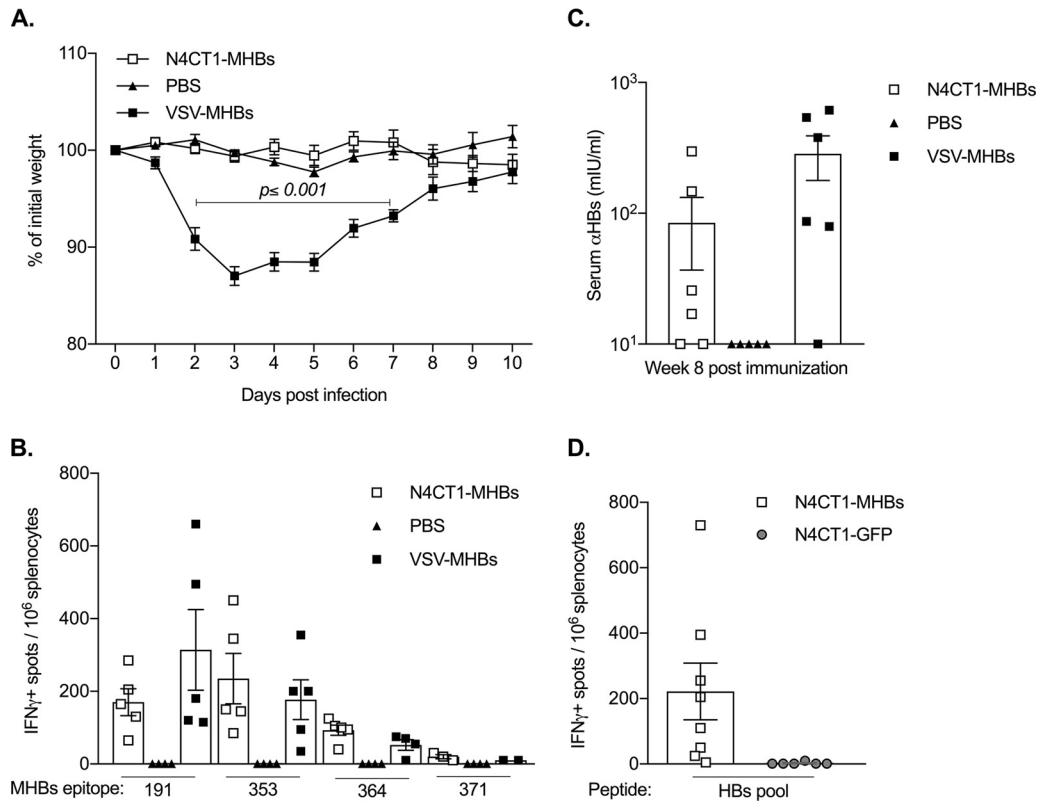


FIG 2 Despite differences in pathogenicity, N4CT1-MHBs and VSV-MHBs generate similar immune responses in naive mice. (A) Daily weight changes of CB6F1 mice infected intranasally with either N4CT1-MHBs or VSV-MHBs (1×10^6 PFU). (B) Ag-specific CD8⁺ T cells measured by an IFN- γ ELISPOT assay in the spleens of CB6F1 mice immunized with the vectors (1×10^6 PFU, i.m.) or PBS on day 7 postimmunization ($n = 5$ mice/group). (C) Anti-HBs antibody measured by an ELISA in CB6F1 mouse serum on week 8 postimmunization ($n = 5$ to 6 mice/group). (D) Ag-specific CD8⁺ T cells measured by an IFN- γ ELISPOT assay in the spleens of DO mice at 2 weeks postimmunization ($n = 6$ to 8 mice/group). Error bars denote SEM.

used Diversity Outbred (DO) mice that mimic the genetic diversity of the human population (21). Induction of Ag-specific T cells in the spleen of DO mice immunized with N4CT1-MHBs was confirmed at 2 weeks postimmunization (Fig. 2D). Thus, despite the lower replicative capacity *in vitro* and diminished pathogenesis *in vivo*, the attenuated N4CT1-MHBs vector generates cellular and humoral immune responses similar to those of a nonattenuated VSV-based vector.

Immunization with N4CT1-MHBs protects mice against hydrodynamic challenge with HBV. To determine whether the T cell responses induced by N4CT1-MHBs immunization in naive mice could control HBV replication, CB6F1 mice were immunized with either N4CT1-MHBs or VSV-MHBs and challenged 6 weeks later by hydrodynamic injection of a plasmid encoding a 1.3-mer copy of the HBV genome (22). Similar to immunization with VSV-MHBs, N4CT1-MHBs immunization prevented HBV replication, as shown by rapid HBeAg clearance from the serum (Fig. 3A) and viral nucleic acid reduction in the liver (Fig. 3B). In contrast to the control group that displayed peak serum HBsAg levels of 820 ± 80 ng/ml at day 4 postchallenge, no HBsAg was detected in the blood of VSV-MHBs- or N4CT1-MHBs-infected mice, consistent with the ability of the vectors to induce anti-HBs antibody in naive animals. Increased liver CD8 expression in both immunized groups suggested the recruitment of Ag-specific CD8⁺ T cells into the liver (Fig. 3C). Induction of HBV-specific CD8⁺ T cells in the spleen was confirmed by a gamma interferon (IFN- γ) enzyme-linked immunosorbent spot (ELISPOT) assay on day 7 postchallenge (Fig. 3D). Thus, N4CT1-MHBs immunization of naive animals induces HBV-specific CD8⁺ T cells that can control virus replication upon subsequent challenge with HBV.

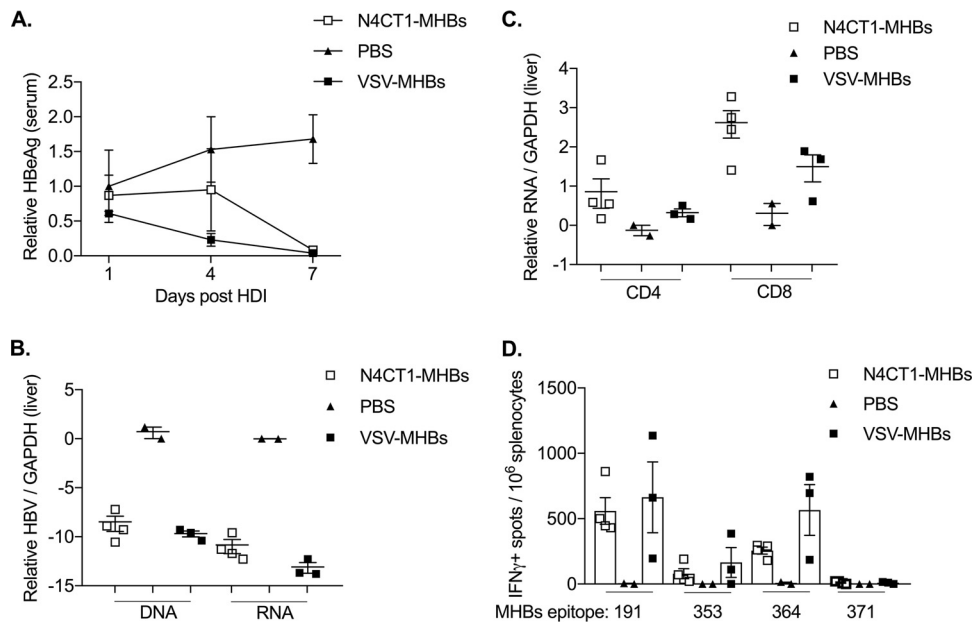


FIG 3 Immunization with N4CT1-MHBs protects mice against HBV hydrodynamic challenge. CB6F1 mice were immunized intramuscularly with 1×10^6 PFU of VSV-MHBs or N4CT1-MHBs and challenged 6 weeks later by hydrodynamic injection (HDI) of the pHBV1.3 plasmid. (A) HBeAg levels measured by an ELISA relative to those in the unimmunized group at day 1 (mean concentration, 307 ± 179 ng/ml) in sera collected on the indicated days postchallenge. (B) Hepatic HBV DNA and RNA on day 7 postchallenge quantified by qPCR and RT-qPCR, respectively, shown as changes in threshold cycle values. (C) Relative liver CD4 and CD8 mRNA quantified by RT-qPCR. (D) HBV-specific CD8⁺ T cell response in the spleen on day 7 postchallenge measured by an IFN- γ ELISPOT assay ($n = 2$ to 4 mice/group). Error bars denote SEM.

Immunization with N4CT1-MHBs elicits Ag-specific immune responses that prevent acute HBV replication in mice.

A mouse model of persistent HBV replication by hepatic transduction of the HBV genome with adeno-associated virus serotype 8 (AAV8) was recently described (20, 23). We utilized the AAV-HBV transduction model to further evaluate the preventative and therapeutic efficacy of N4CT1-MHBs in mice. To test the preventative effects of N4CT1-MHBs, CB6F1 mice were immunized with either N4CT1-MHBs, VSV-MHBs, N4CT1-GFP, or phosphate-buffered saline (PBS) and 6 weeks later were challenged intravenously (i.v.) with 1×10^{11} genome copies of AAV-HBV. HBV replication was monitored by detection of viral Ags in the serum and nucleic acids in the liver. Immunization with N4CT1-MHBs or VSV-MHBs reduced serum HBsAg starting from week 1 postchallenge, which continued up to week 4 postchallenge (Fig. 4A). HBsAg clearance after challenge in the immunized groups is likely due to anti-HBs antibody induced by the immunizations. In both immunized groups, anti-HBs antibody was detected by an ELISA in sera prior to challenge and continued to increase by week 4 postchallenge (Fig. 4B). As expected, no serum anti-HBs Ab was detected in the negative-control groups prior to challenge; however, starting from week 3 postchallenge, a reduced serum HBsAg level in some negative-control mice was observed that was associated with detectable serum anti-HBs Ab at week 4, which was significantly lower than that in the immunized groups (Fig. 4A and B). Anti-HBs Ab development in negative-control groups might be due to the BALB/c major histocompatibility complex (MHC) proteins in CB6F1 mice, as it has been reported that hydrodynamic injection of an AAV-HBV plasmid resulted in the development of anti-HBs in 100% of male BALB/c mice by week 2 postinjection (24). Since HBV virions are not able to reinfect mouse hepatocytes, the presence of anti-HBs in the serum might prevent HBsAg detection by an ELISA but not have any effect on the amount of virus in the liver. Therefore, serum HBeAg, for which we did not detect either preexisting or vaccine-induced antibody, was also measured by an ELISA. While no significant difference was observed in serum HBeAg levels in both immunized and negative-control groups on week 1 postchal-

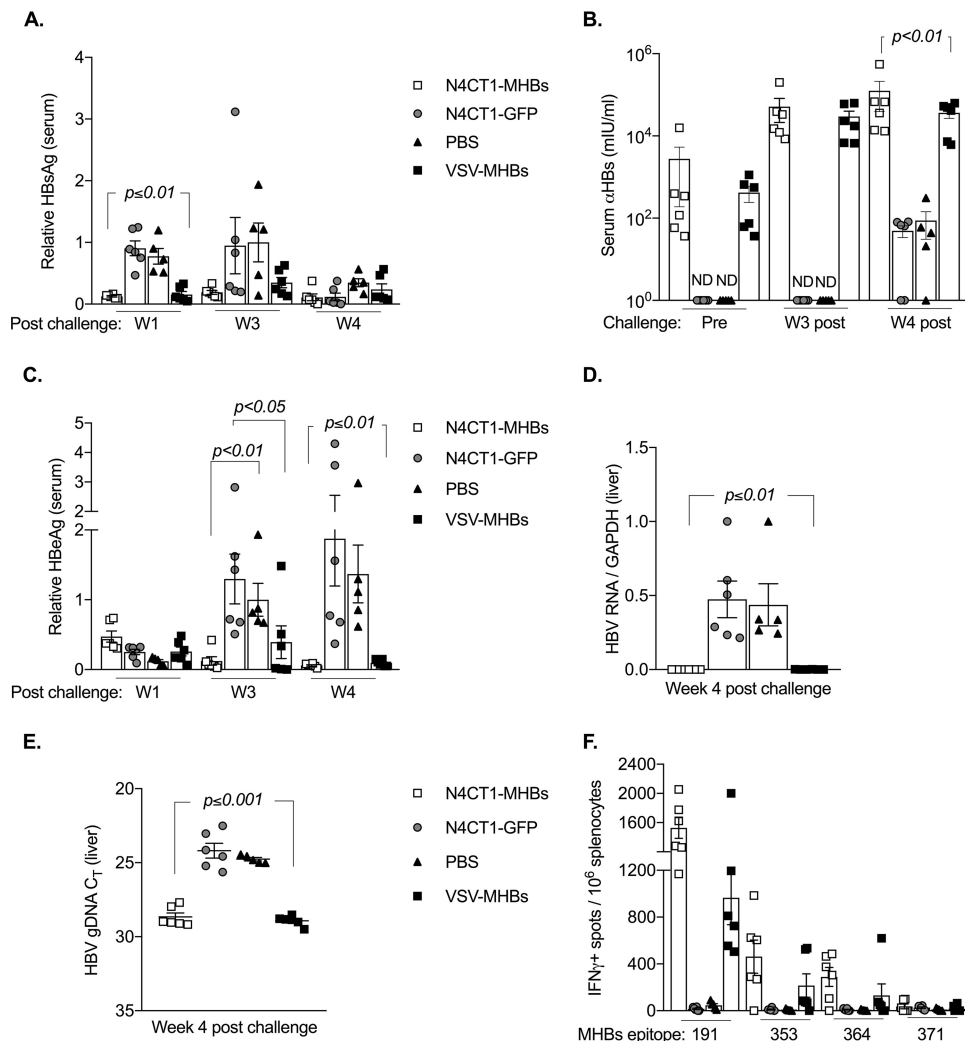


FIG 4 Immunization with N4CT1-MHBs elicits Ag-specific immune responses that prevent persistent HBV replication in mice. CB6F1 mice were immunized with the indicated vectors (1×10^6 PFU, i.m.) and challenged i.v. with 1×10^{11} genome copies of AAV-HBV at week 6 postimmunization. (A) Serum HBsAg levels measured by ELISAs relative to those in the week 3 postchallenge PBS group (mean concentration, 48 ± 23 ng/ml). (B) Anti-HBs quantification by an ELISA in serum prior to challenge (pre) and at week 3 (W3) and week 4 postchallenge. (C) Serum HBeAg levels measured by an ELISA relative to those in the week 3 postchallenge PBS group (mean concentration, 79 ± 7 ng/ml). (D and E) Hepatic HBV RNA and genomic DNA (gDNA) levels on week 4 postchallenge measured by RT-qPCR and qPCR, respectively. C_T , threshold cycle. (F) MHBs-specific CD8 $^+$ T cell detection by an IFN- γ ELISPOT assay in the spleen on week 4 postchallenge ($n = 5$ to 6 mice/group). Error bars denote SEM.

allenge, a significant HBeAg reduction was observed at weeks 3 and 4 postchallenge in immunized groups compared to the negative controls (Fig. 4C).

The reduction in HBeAg is consistent with the possible presence of a cell-mediated immune response that could prevent virus replication in the MHBs-immunized groups. To examine this possibility, viral RNA and DNA in the liver at week 4 postchallenge were measured by reverse transcription-quantitative PCR (RT-qPCR) and qPCR, respectively, which demonstrated that immunization with either N4CT1-MHBs or VSV-MHBs prevented the establishment of persistent HBV gene expression and DNA production in the liver (Fig. 4D and E). Because HBV Ag recognition by CD8 $^+$ T cells triggers the release of antiviral cytokines such as IFN- γ and tumor necrosis factor alpha (TNF- α) that inhibit virus replication (25, 26), we performed an IFN- γ ELISPOT assay using spleen cells to detect the presence of functional HBV-specific CD8 $^+$ T cells. IFN- γ -producing MHBs-specific CD8 $^+$ T cells were found in the spleens of mice immunized with N4CT1-MHBs or VSV-MHBs, while no Ag-specific CD8 $^+$ T cells were found in mice immunized with

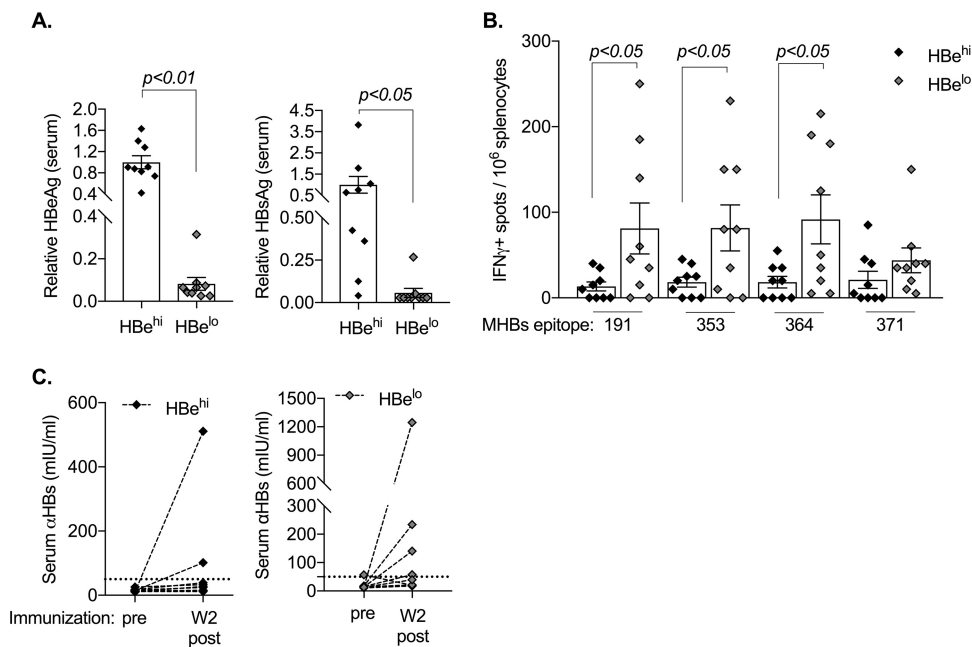


FIG 5 Immunization with N4CT1-MHBs overcomes immune tolerance in HBV^{tg} mice. (A) Measurement of serum HBeAg (left) and HBsAg (right) in HBV.CB6F1 mice by an ELISA. (B) HBV-specific CD8⁺ T cells in the spleen at week 2 postimmunization. (C) Anti-HBs Ab levels in the serum before immunization (pre) and at week 2 postimmunization. The assay limit of detection is shown by a dotted line ($n = 9$ mice/group). Error bars denote SEM.

N4CT1-GFP or PBS (Fig. 4F). Therefore, a single immunization with N4CT1-MHBs generates effective antibody and CD8⁺ T cell responses that protect mice against subsequent HBV challenge and prevent virus replication in the liver.

Immunization with N4CT1-MHBs induces CD8⁺ T cell responses in HBV transgenic mice. We have shown previously that immunization of highly tolerant HBV^{tg} mice with VSV-MHBs induces HBV-specific CD8⁺ T cells in mice that naturally express low levels of antigen (12). To evaluate the ability of N4CT1-MHBs to overcome immune tolerance in HBV^{tg} mice, HBeAg^{lo} and HBeAg^{hi} HBV.CB6F1 mice (Fig. 5A) were immunized with N4CT1-MHBs. A significantly higher frequency of HBV-specific CD8⁺ T cells was observed in the spleens of HBeAg^{lo} mice than in HBeAg^{hi} mice at week 2 posttreatment (Fig. 5B). N4CT1-MHBs immunization also resulted in the generation of anti-HBs antibody in a subset of the mice (Fig. 5C). Therefore, similar to nonattenuated VSV, N4CT1-MHBs immunization is able to overcome immune tolerance in HBV^{tg} mice.

N4CT1-MHBs immunization of mice with persistent HBV replication results in significant serum viral Ag reduction and MHBs-specific CD8⁺ T cell induction. To investigate the therapeutic effect of N4CT1-MHBs in the AAV mouse model of persistent HBV replication, C57BL/6 mice were transduced with AAV-HBV and monitored weekly for serum HBeAg and HBsAg levels. On week 8 posttransduction, three groups of HBsAg-matched mice were treated with either N4CT1-MHBs, N4CT1-GFP, or PBS. The relative Ag levels in the serum were normalized between the three groups at week 8 after AAV-HBV transduction and compared at weeks 1 to 3 posttreatment (Fig. 6A and B). A significant reduction in serum HBsAg and HBeAg was observed starting from week 2 posttreatment in mice infected with N4CT1-MHBs compared to the control groups and continued up to week 3 posttreatment, when the mice were euthanized for analysis of their immune responses. Because we failed to detect anti-HBs antibody in the serum, this suggests that the reduction in antigenemia is due to T cell-mediated mechanisms. Consistent with this hypothesis, N4CT1-MHBs treatment elicited significantly higher MHBs-specific CD8⁺ T cell numbers in the spleen, as measured by an IFN- γ ELISPOT assay, while responses in both control groups were not significantly higher than the background (Fig. 6C). Furthermore, the reduction in antigenemia was

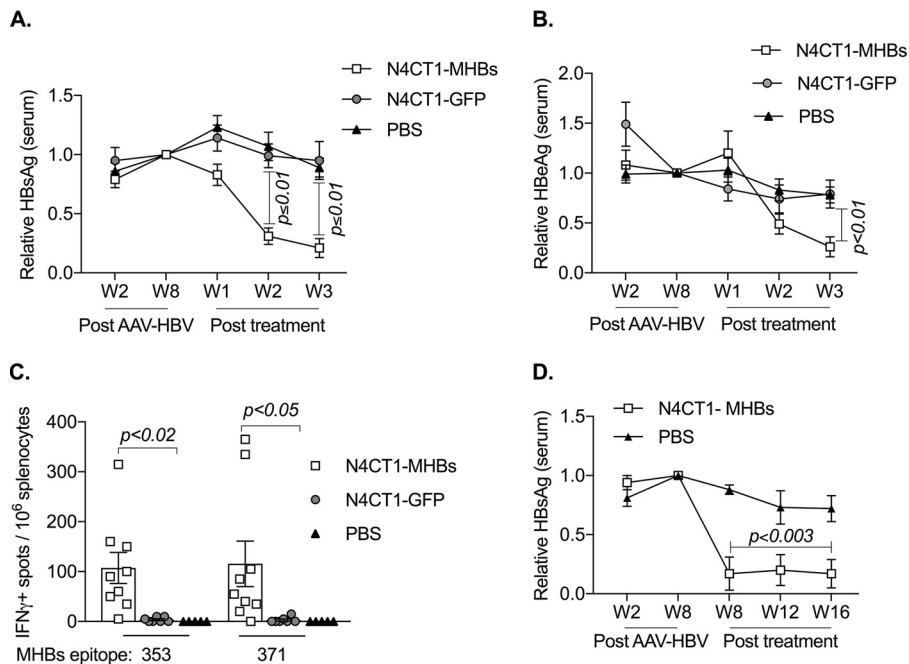


FIG 6 N4CT1-MHBs treatment of mice with persistent HBV replication results in significant HBV Ag reduction and Ag-specific CD8⁺ T cell induction. C57BL/6 mice received 1×10^{11} genome copies of AAV-HBV i.v. and on week 8 posttransduction were treated with the indicated vectors (1×10^6 PFU, i.m.) or PBS. (A and B) Serum HBV Ag levels at different time points measured by an ELISA relative to those on week 8 after AAV-HBV transduction. The mean concentrations \pm SEM of serum HBsAg and HBeAg at the time of treatment were 182 ± 11 and 94 ± 9 ng/ml, respectively. (C) IFN- γ ELISPOT analysis of MHBs-specific CD8⁺ T cell responses in the spleen on week 3 posttreatment. (D) Serum HBsAg levels at different time points measured by an ELISA relative to those at week 8. The mean concentration of HBsAg at the time of treatment was 296 ± 36 ng/ml ($n = 5$ to 9 mice/group). Error bars denote SEM.

lasting and lasted at least 16 weeks posttreatment in an additional longer-term experiment (Fig. 6D). These results indicate that a single treatment with N4CT1-MHBs overcomes T cell dysfunction and induces cell-mediated immune responses in this model.

N4CT1-MHBs treatment of mice with persistent HBV infection reduces hepatic HBV replication forms. To better quantify the CD8⁺ T cell induction kinetics and HBV replication in the liver, mice with established persistent HBV replication were treated with N4CT1-MHBs or N4CT1-GFP, and groups of animals were euthanized at 1, 3, or 5 weeks posttreatment to examine T cell responses in the spleen and HBV replication forms in the liver. A single treatment with N4CT1-MHBs resulted in a marked serum HBeAg and HBsAg decline starting at week 3 posttreatment and continuing through week 5 posttreatment (Fig. 7A and B). MHBs-specific CD8⁺ T cells expressing IFN- γ were detected by ELISPOT assays in the spleens of mice treated with N4CT1-MHBs starting at week 1 posttreatment, and their numbers continued to increase through week 5 (Fig. 7C). N4CT1-MHBs-treated mice showed a significant but transient increase in serum alanine aminotransferase (ALT) activity beginning at week 2 posttreatment and continuing to week 4 posttreatment before declining afterward (Fig. 7D). The increase in serum ALT activity correlated with increased liver CD8 expression in mice treated with N4CT1-MHBs, while no significant increase in CD4 expression was observed (Fig. 7E). A significant reduction in HBV RNA and DNA in the liver of mice treated with N4CT1-MHBs but not N4CT1-GFP was observed (Fig. 7F), which directly correlated with the reduction of viral Ags in the serum and inversely correlated with the induction of MHBs-specific T cells in the spleen, increased CD8 expression in the liver, and elevation of serum ALT activity. To further confirm the correlation between HBV reduction and the induction of an effective HBV-specific T cell response in the liver, two additional groups of mice with established persistent HBV replication were treated with either N4CT1-MHBs or PBS,

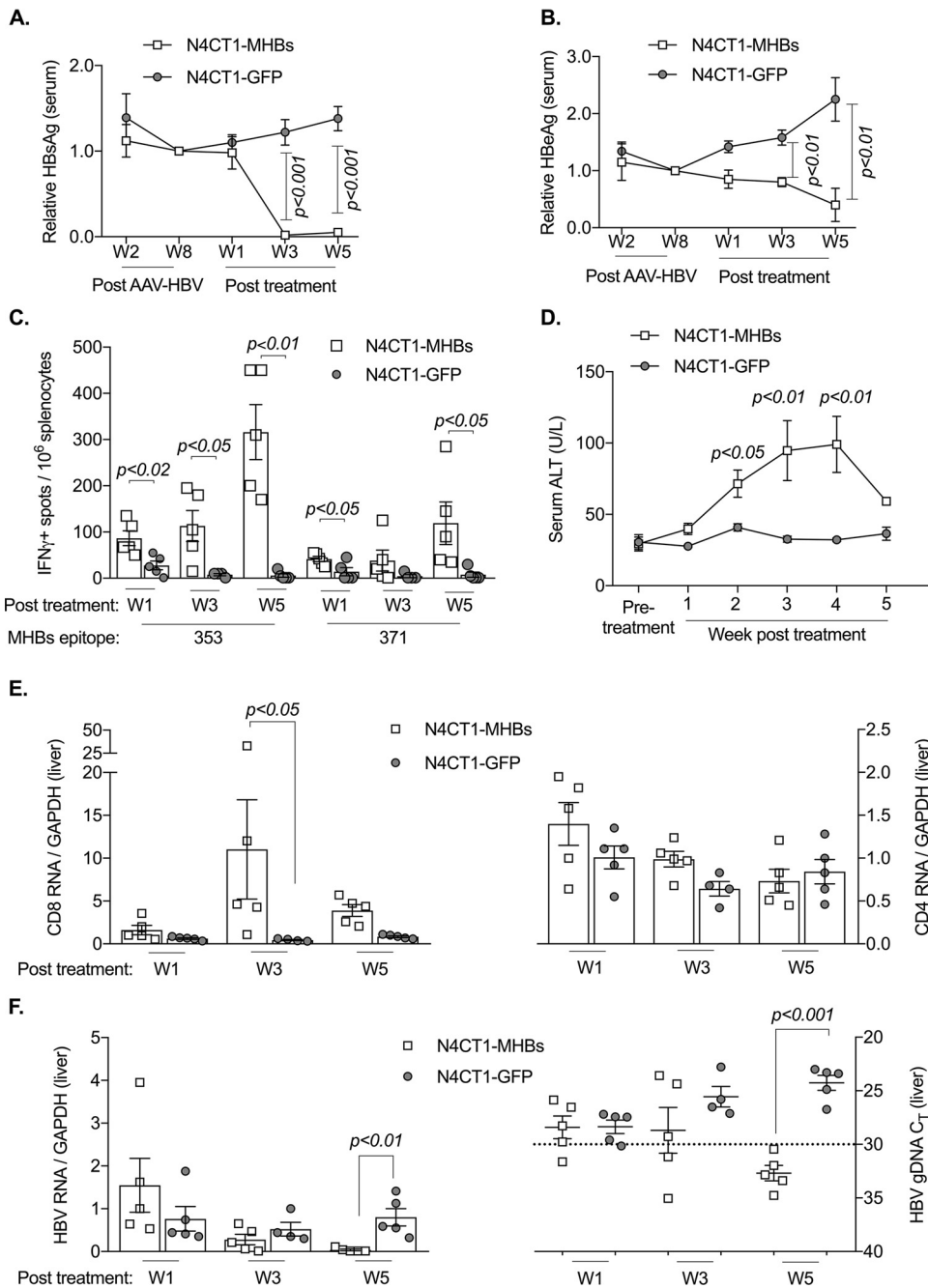


FIG 7 A single treatment by N4CT1-MHBs in mice with persistent HBV replication results in viral Ag clearance from serum, reduced viral replication in the liver, transient ALT elevation, and increased Ag-specific CD8⁺ T cell frequency. C57BL/6 mice received 1×10^{11} genome copies of AAV-HBV i.v. and on week 8 posttransduction were treated with the indicated vectors (1×10^6 PFU i.m.). (A and B) Serum viral Ag levels at different time points measured by an ELISA relative to those on week 8 after AAV-HBV transduction. The concentrations \pm SEM of serum HBsAg and HBeAg at the time of treatment were 166 ± 17 and 106 ± 7 ng/ml, respectively. (C) IFN- γ ELISPOT analysis of MHBs-specific CD8⁺ T cells in the spleens of mice at different weeks posttreatment. (D) Serum ALT activity before treatment and at the indicated weeks posttreatment. (E) Liver CD8 and CD4 mRNA expression measured by RT-qPCR. (F) Relative hepatic HBV RNA (normalized to GAPDH) and HBV genomic DNA (in 50 mg of liver tissue) quantified by RT-qPCR and qPCR, respectively. Background PCR amplification (limit of detection) in nontransduced mouse livers is shown by a dotted line. Data shown in panels A, B, and D are derived from two groups of mice that were euthanized on week 5 posttreatment, and data shown in panels C and E to G are from two groups of mice euthanized at the indicated time points ($n = 5$ mice/group). Error bars denote SEM.

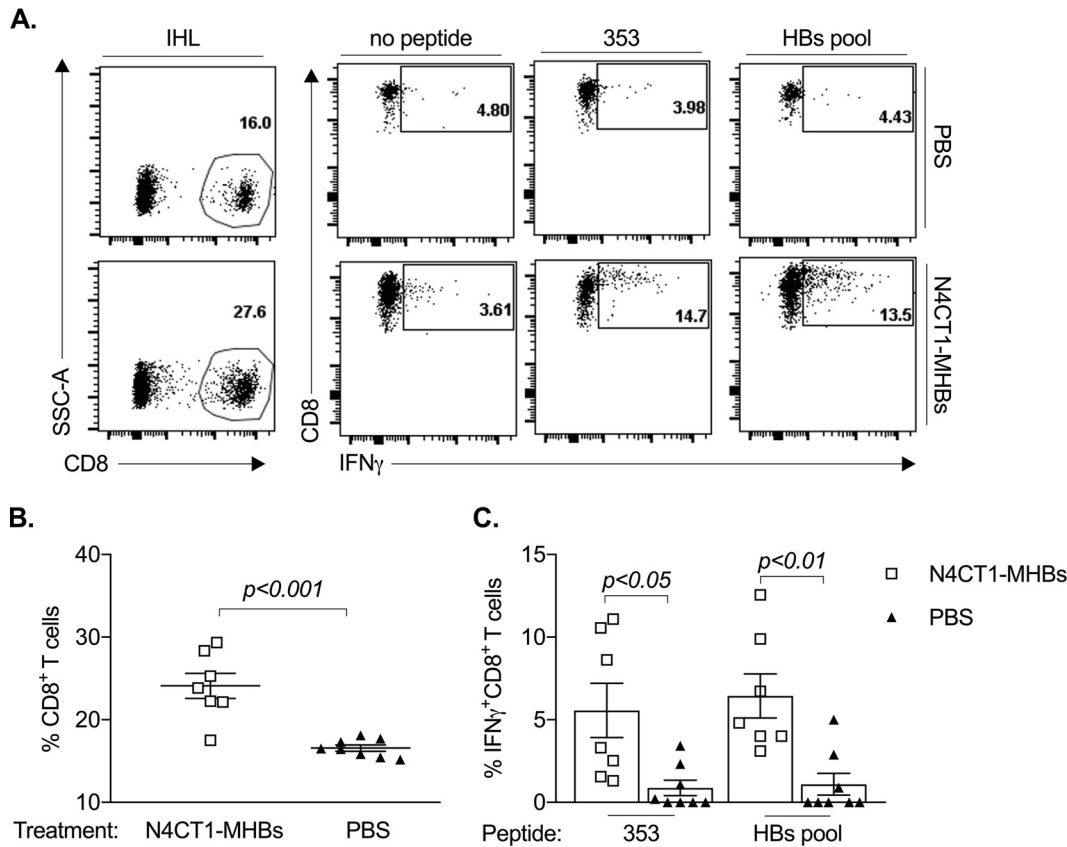


FIG 8 Increased frequency of HBV-specific CD8⁺ T cells in the livers of mice treated with N4CT1-MHBs. AAV-HBV-transduced C57BL/6 mice with persistent HBV replication were treated with N4CT1-MHBs (1×10^6 PFU i.m.) or PBS. IHL were isolated at week 3 posttreatment, stimulated overnight in the presence or absence of HBV peptides, and stained for expression of CD8 and IFN- γ . (A) Representative flow cytometry plots of IHL. SSC, side scatter. (B) Frequency of CD8⁺ T cells among IHL. (C) Frequency of HBV-specific CD8⁺ IFN- γ ⁺ cells among IHL after *in vitro* stimulation with HBV peptides.

and on week 3 posttreatment, intrahepatic lymphocytes (IHL) were isolated and stimulated with HBV peptides. Flow cytometry analysis (Fig. 8) showed that N4CT1-MHBs treatment resulted in not only a significant increase in the frequency of hepatic CD8⁺ T cells but also an increase in the frequency of HBV-specific CD8⁺ IFN- γ ⁺ T cells. Therefore, N4CT1-MHBs immunization of mice with established HBV infection elicits HBV-specific T cell responses that can control HBV replication in the liver.

DISCUSSION

Immune system dysfunction in chronic HBV patients has been attributed to exhaustion and/or deletion of HBV-specific CD8⁺ T cells (27). Acute HBV infection resolution in adults and serum HBsAg clearance in chronic HBV patients following hematopoietic stem cell transplantation (28), along with spontaneous infection resolution in some patients (4), all suggest that chronic HBV cure might be attainable by strategies such as therapeutic vaccination with the aim of boosting adaptive immune responses and rejuvenating HBV-specific CD8⁺ T cells. Although we focus here on the MHBs protein as the antigen for immunization, effective control of HBV infection in humans will likely require broad multispecific immune responses to several HBV antigens. Even though there is no clear consensus as to which antigen might be most effective therapeutically, preclinical studies in the woodchuck hepatitis virus model have demonstrated that core-specific T cell responses may be particularly valuable (29–31).

Live attenuated, replicating viral platforms that generate long-lasting protective cellular and humoral immune responses might offer a new tool for chronic HBV treatment. A main concern regarding the use of replicating vaccine platforms is the

balance between safety and efficacy, so the trade-off between vector attenuation and immunogenicity is critical (32). In addition to eliciting mucosal and systemic immune responses and efficiently inducing CD8⁺ T cells, VSV has other advantages, including ease of propagation, low preexisting immunity, broad tissue tropism, no risk of integration into the host genome, ease of genetic manipulation, high level of antigen expression, and availability in different serotypes for boosting (9, 33).

In this study, we determined the immunogenicity and efficacy of a highly attenuated VSV-based vector in controlling HBV replication and overcoming immune tolerance in different immunocompetent mouse models of HBV replication. Our results demonstrated that a single immunization with N4CT1-MHBs induces HBV-specific CD8⁺ T cell responses that protect mice against further challenge in acute HBV replication models. In addition, infection of HBV transgenic mice with N4CT1-MHBs elicited functional HBV-specific CD8⁺ T cells. Although HBV transgenic mice have been used as a chronic HBV infection model to evaluate the efficacy of experimental vaccines (12, 34–37), the presence of the integrated transgene in these mice does not allow the measurement of HBV clearance. A recently developed AAV-HBV transduction model (20, 23) enables persistent viral replication, the production of physiologically relevant levels of HBV antigens, and the development of immune tolerance and has been used recently for evaluating different therapeutic approaches (23, 38–42). HBV vaccines combined with immunomodulation such as depleting HBsAg (39, 40) or using adjuvants (20, 39, 41), as well as a nonreplicating viral vector (38), have shown some efficacy in inducing HBV-specific T cells in the AAV-HBV transduction model.

In line with previous studies using the model, N4CT1-MHBs treatment of AAV-HBV-transduced mice resulted in a significant induction of Ag-specific IFN- γ -expressing CD8⁺ T cells. We focused on the ability of N4CT1-MHBs to elicit HBV-specific CD8⁺ T cells because of the well-known role of these cells in the effective resolution of HBV infection. Although in this study we did not directly investigate Ag-specific CD8⁺ T cell cytolytic activity, the simultaneous transient increase in serum ALT activity and liver CD8 expression along with the increased frequency of intrahepatic CD8⁺ IFN- γ ⁺ T cells and elimination of viral nucleic acids following N4CT1-MHBs administration all suggest ongoing cytolytic activity that is most likely related to Ag-specific CD8⁺ T cells. Further understanding the mechanism(s) involved in activating functional Ag-specific CD8⁺ T cells in mice with persistent HBV replication is worthy of additional study. In particular, the roles of T cell tolerance, exhaustion, and the absence of initial priming in promoting virus persistence in the AAV-HBV model have not been completely defined.

It will also be important to understand the contribution of other immune cell types to vaccine-induced CD8⁺ T cell responses. For example, CD4⁺ T cells contribute to the differentiation and maintenance of memory CD8⁺ T cells (43) and their mobilization into virus-infected tissues (44). More recently, aberrant differentiation and exhaustion of CD8⁺ T cells primed with viral vectors in the absence of CD4⁺ T cells have been reported (45). Although we did not observe a significant increase in liver CD4 expression in mice treated with N4CT1-MHBs, it is possible that CD4⁺ T cells also play an important role in the modulation of Ag-specific CD8⁺ T cell activity in this model. These could be either helper T cells that support CD8⁺ T cell activation or regulatory T cells that suppress immune responses in the liver and promote tolerance. Moreover, CD8⁺ T cell responses might also be influenced by NK cells, which modulate T cell responses via direct or indirect mechanisms (46). For example, in patients with chronic HBV infection, NK cells negatively regulate HBV-specific CD8⁺ T cells in a TRAIL-R2-dependent manner (47).

One limitation of our study relates to the level of antigen present in the AAV-HBV-transduced mice at the time of N4CT1-MHBs immunization, which was lower than the levels previously achieved in other studies using this model (23, 38, 42, 48). This could be due to differences in the HBV genome insert (1.3-mer versus 1.2-mer) or the infectious titer of the vectors. Although a previous study demonstrated the therapeutic efficacy of a vaccine platform that was independent of pretreatment HBsAg levels (42), it is likely that T cell dysfunction in the context of relatively low HBV antigen levels is

easier to overcome through therapeutic immunization. This notion is also evident in our studies using HBV transgenic mice, in which MHBs-specific T cell responses were more readily detected in mice expressing low HBV antigen levels. Additional studies will be needed to better understand how the association between antigenemia and T cell dysfunction in the AAV-HBV model accurately reflects human chronic HBV infection and how vaccine-induced immune effectors such as CD8⁺ T cells and antibody contribute to virus control. Despite observing a significant HBsAg reduction in serum, we were not able to detect anti-HBs in serum of AAV-HBV-transduced mice after treatment with N4CT1-MHBs, which might be due to the limitation of the detection assay. Alternatively, it is possible that abundant HBsAg release in serum resulted in the occupation of all the antibody complementarity-determining regions and prevented its detection by ELISAs.

In summary, the results of this study show that a single dose of highly attenuated VSV can induce Ag-specific T cells, prevent the establishment of persistent HBV replication, and control virus replication in mice with persistent HBV infection. These results warrant more-detailed investigation of the functional mechanisms of highly attenuated virus-based vaccine platforms in HBV-specific T cell activation in AAV-HBV-transduced mice and other animal models of chronic HBV infection.

MATERIALS AND METHODS

Animals. Mice were maintained in the AAALAC-accredited Animal Resource Facility at Albany Medical College (AMC) and were handled with procedures approved by the AMC Institutional Animal Care and Use Committee. C57BL/6 and BALB/c mice were purchased from The Jackson Laboratory or Taconic Biosciences. C57BL/6 × BALB/c F1 (CB6F1) mice were bred in the AMC Animal Resource Facility or purchased from The Jackson Laboratory. HBV transgenic (HBV^{tg}) mice (strain 1.3.32) on the C57BL/6 background were originally produced in the laboratory of Francis V. Chisari at The Scripps Research Institute (49). Strain 1.3.32 × BALB/c F1 mice (HBV.CB6F1) were bred in the AMC Animal Resource Facility. Diversity Outbred (DO) mice were purchased from The Jackson Laboratory (stock number 009376). Male mice at 8 to 10 weeks of age were used for all experiments.

Recombinant VSV vectors. VSV-MHBs construction was described previously (11). To generate the N4CT1-MHBs virus, a 5,725-bp DNA sequence encoding the HBV MHBs protein (serotype ayw) flanked by XhoI and NotI sites followed by the VSV P-M-N-G-L genes, as described previously (13, 14), was synthesized by GenScript. A termination codon was included in the G open reading frame to remove the carboxy-terminal 28 amino acids of the protein. An XhoI-HpaI fragment encoding the MHBs-P-M-N-G_{CT1}-L sequence was inserted into the pVSV1XN plasmid (50). Control N4CT1-GFP virus was generated by replacing MHBs with the GFP coding sequence between the XhoI and NotI sites. Recombinant viruses were generated as previously described (50). To confirm recombinant protein expression, the MHBs level was measured in infected BHK-21 cell (American Type Culture Collection) lysates by Western blot analysis using anti-preS2 antibody (Santa Cruz Biotechnology). VSV protein expression was confirmed by Western blotting using anti-VSV polyclonal rabbit serum (51). For virus propagation, BHK-21 cells at 60 to 70% confluence were infected at a multiplicity of infection (MOI) of 0.01, and medium was collected when >90% cytopathic effect was observed. Cells and debris were removed by centrifugation (1,200 rpm at 4°C for 10 min), and the supernatant was used for further virus concentration by ultracentrifugation (25,000 rpm at 4°C for 2 h). The pellet containing the concentrated virus was resuspended in PBS, aliquoted, and stored at -80°C. Virus titers were determined by routine methods. Viruses were diluted in PBS prior to administration of 1 × 10⁶ PFU to mice by either the intranasal (i.n.) or intramuscular (i.m.) route.

AAV-HBV. Adeno-associated virus (capsid serotype AAV8) expressing a 1.3-mer overlength HBV genome (serotype ayw) was purchased from Vector Biolabs and SignaGen. Male C57BL/6 mice were transduced i.v. with 1 × 10¹¹ genome copies of AAV-HBV. Establishment of persistent HBV replication was defined by the presence of similar serum viral antigen (Ag) levels on week 8 compared to those at week 2 after delivery of AAV-HBV.

HBV antigen and antibody ELISA. HBsAg and HBeAg ELISA kits (International Immunodiagnostics) were used to measure HBsAg and HBeAg in mouse sera. Quantification of HBsAg and HBeAg was performed using known concentrations of HBsAg and HBeAg proteins (Fitzgerald Industries International) diluted in normal mouse serum. An HBs Ab quantitative ELISA kit (International Immunodiagnostics) was used to quantify anti-HBs antibody.

IFN-γ ELISPOT assay. Mouse CD8⁺ T cell epitopes in MHBs were described previously (11). Peptides with >95% purity were provided by GenScript. In experiments with CB6F1 mice, four MHBs CD8⁺ T cell epitopes (positions 191 to 202 relative to the first amino acid of the large surface protein, IPQSLDSWW TSL, L^d; positions 353 to 360, VWLSVIWM, K^b; positions 364 to 372, WGPLSYLSIL, D^d; and positions 371 to 378, ILSPFLPL, K^b) were examined to analyze both H-2^b- and H-2^d-specific responses. For experiments with C57BL/6 mice, only the two H-2^b-specific epitopes (positions 353 to 360 and 371 to 378) were used. In some experiments, a pool of HBV surface glycoprotein genotype D peptides (15-mers with an 11-amino-acid overlap; GenScript) (HBs pool) was utilized. ELISPOT assays were performed according to a previously described protocol (52).

Serum alanine aminotransferase activity. Serum ALT activity was measured with a SpectraMax 190 microplate reader (Molecular Devices) using Infinity ALT liquid stable reagent (Thermo Scientific) and Enzyme ER verifier kit standards (Verichem Laboratories).

HBV RNA expression and measurement of gene expression. Liver tissue was snap-frozen in liquid nitrogen and stored at -80°C for homogenization and RNA and DNA purification. Total RNA was prepared using the RNeasy Plus minikit (Qiagen). Equal amounts of total RNA from each sample were used for cDNA preparation with a high-capacity cDNA reverse transcription kit (Applied Biosystems). Quantitative RT-PCR was performed using TaqMan Fast advanced master mix (Applied Biosystems) and TaqMan assay mix containing a probe and specific primers for each gene. Glycerinaldehyde-3-phosphate dehydrogenase (GAPDH) was used as an endogenous control, qPCR was performed on a StepOnePlus real-time PCR system (Applied Biosystems) using StepOne software v2.3, and gene expression was quantified by the comparative $\Delta\Delta C_T$ method.

Liver DNA preparation and HBV detection. Capsid-associated HBV DNA was purified from mouse livers according to a modified protocol described previously (53). Fifty milligrams of frozen liver tissue was homogenized in 1 ml cell lysis buffer (50 mM Tris [pH 7.5], 0.5% NP-40, 1 mM EDTA, and 100 mM NaCl) and incubated for 1 h at 4°C , after which 10 mM MgCl_2 and 200 μg DNase I were added. Following a 3-h incubation at 37°C , 25 mM EDTA and 250 μl of 35% polyethylene glycol 8000 were added, and the mixture was incubated on ice for 30 min, followed by a 30-min centrifugation at 13,000 rpm to precipitate and concentrate viral capsids. The pellet was resuspended in lysis buffer (10 mM Tris, 100 mM NaCl, 1 mM EDTA, and 1% SDS) with 250 μg proteinase K and incubated overnight at 37°C . Viral DNA was purified by phenol-chloroform extraction followed by isopropanol precipitation. The precipitated DNA was washed in 70% ethanol (EtOH), and the dried pellet was resuspended in Tris-EDTA. HBV genomes were detected by quantitative PCR using the following probe and primers (54): HBV probe FAM (6-carboxyfluorescein)-5'-CCT CTT CAT CCT GCT GCT ATG CCT CAT C-3'-MGBNFQ (minor groove binder nonfluorescent quencher), forward primer 5'-GTG TCT GCG GCG TTT TAT CA-3', and reverse primer 5'-GAC AAA CGG GCA ACA TAC CTT-3'. Liver samples from HBV transgenic mice and naive C57BL/6 mice were used as positive and negative controls, respectively.

Flow cytometry staining of intrahepatic lymphocytes. Livers were perfused with PBS and dissociated by passage through a nylon mesh strainer, and cells were resuspended in 40% isotonic Percoll in serum-free medium and centrifuged at $600 \times g$ for 20 min at room temperature. IHL were collected and, after red blood cell lysis, were used for *in vitro* stimulation with HBV peptides overnight. Brefeldin A and monensin were added 5 h prior to surface staining of the cells with anti-mouse CD8 α (eBioscience) and subsequent intracellular staining with anti-mouse IFN- γ (eBioscience). Samples were analyzed on an LSRII flow cytometer (BD Biosciences).

Statistical analysis. All data were analyzed using GraphPad Prism software (version 7). Depending on the type of experiment, either paired, unpaired, or multiple *t* tests were performed to determine significance ($P < 0.05$).

ACKNOWLEDGMENTS

We thank Linda Buonocore and Tracy Reynolds for discussions and technical assistance.

Research reported in this publication was supported by the State of Connecticut Department of Public Health under award number 2014-0137 and the National Institute of Allergy and Infectious Diseases of the National Institutes of Health under award numbers R01AI124006 and R21AI109410. The content is solely the responsibility of the authors and does not necessarily represent the official views of the Connecticut Department of Public Health or the National Institutes of Health.

REFERENCES

- World Health Organization. 2018. Hepatitis B fact sheet. World Health Organization, Geneva, Switzerland. <http://www.who.int/mediacentre/factsheets/fs204/en/>.
- Nassal M. 2015. HBV cccDNA: viral persistence reservoir and key obstacle for a cure of chronic hepatitis B. *Gut* 64:1972–1984. <https://doi.org/10.1136/gutjnl-2015-309809>.
- Nebbia G, Peppia D, Maini MK. 2012. Hepatitis B infection: current concepts and future challenges. *QJM* 105:109–113. <https://doi.org/10.1093/qjmed/hcr270>.
- Han ZG, Qie ZH, Qiao WZ. 2016. HBsAg spontaneous seroclearance in a cohort of HBeAg-seronegative patients with chronic hepatitis B virus infection. *J Med Virol* 88:79–85. <https://doi.org/10.1002/jmv.24311>.
- Kutscher S, Bauer T, Dembek C, Sprinzl M, Protzer U. 2012. Design of therapeutic vaccines: hepatitis B as an example. *Microb Biotechnol* 5:270–282. <https://doi.org/10.1111/j.1751-7915.2011.00303.x>.
- Dembek C, Protzer U, Roggendorf M. 2018. Overcoming immune tolerance in chronic hepatitis B by therapeutic vaccination. *Curr Opin Virol* 30:58–67. <https://doi.org/10.1016/j.coviro.2018.04.003>.
- Fontaine H, Kahi S, Chazallon C, Bourguine M, Varaut A, Buffet C, Godon O, Meritet JF, Saïdi Y, Michel ML, Scott-Algara D, Aboulker JP, Pol S, ANRS HB02 Study Group. 2015. Anti-HBV DNA vaccination does not prevent relapse after discontinuation of analogues in the treatment of chronic hepatitis B: a randomised trial—ANRS HB02 VAC-ADN. *Gut* 64:139–147. <https://doi.org/10.1136/gutjnl-2013-305707>.
- Bertoletti A, Gehring AJ. 2013. Immune therapeutic strategies in chronic hepatitis B virus infection: virus or inflammation control? *PLoS Pathog* 9:e1003784. <https://doi.org/10.1371/journal.ppat.1003784>.
- Clarke DK, Cooper D, Egan MA, Hendry RM, Parks CL, Udem SA. 2006. Recombinant vesicular stomatitis virus as an HIV-1 vaccine vector. *Springer Semin Immunopathol* 28:239–253. <https://doi.org/10.1007/s00281-006-0042-3>.
- Henao-Restrepo AM, Camacho A, Longini IM, Watson CH, Edmunds WJ, Egger M, Carroll MW, Dean NE, Diatta I, Doumbia M, Draguez B, Durafour S, Enwere G, Grais R, Gunther S, Gsell P-S, Hossmann S, Watle SV, Kondé MK, Kéïta S, Kone S, Kuisma E, Levine MM, Mandal S, Mauget T, Norheim G, Riveros X, Soumah A, Trelle S, Vicari AS, Røttingen J-A, Kieny

- M-P. 2017. Efficacy and effectiveness of an rVSV-vectored vaccine in preventing Ebola virus disease: final results from the Guinea ring vaccination, open-label, cluster-randomised trial (Ebola Ca Suffit!). *Lancet* 389:505–518. [https://doi.org/10.1016/S0140-6736\(16\)32621-6](https://doi.org/10.1016/S0140-6736(16)32621-6).
11. Cobleigh MA, Buonocore L, Uprichard SL, Rose JK, Robek MD. 2010. A vesicular stomatitis virus-based hepatitis B virus vaccine vector provides protection against challenge in a single dose. *J Virol* 84:7513–7522. <https://doi.org/10.1128/JVI.00200-10>.
 12. Cobleigh MA, Wei X, Robek MD. 2013. A vesicular stomatitis virus-based therapeutic vaccine generates a functional CD8 T cell response to hepatitis B virus in transgenic mice. *J Virol* 87:2969–2973. <https://doi.org/10.1128/JVI.02111-12>.
 13. Clarke DK, Nasar F, Lee M, Johnson JE, Wright K, Calderon P, Guo M, Natuk R, Cooper D, Hendry RM, Udem SA. 2007. Synergistic attenuation of vesicular stomatitis virus by combination of specific G gene truncations and N gene translocations. *J Virol* 81:2056–2064. <https://doi.org/10.1128/JVI.01911-06>.
 14. Cooper D, Wright KJ, Calderon PC, Guo M, Nasar F, Johnson JE, Coleman JW, Lee M, Kotash C, Yurgeloni I, Natuk RJ, Hendry RM, Udem SA, Clarke DK. 2008. Attenuation of recombinant vesicular stomatitis virus-human immunodeficiency virus type 1 vaccine vectors by gene translocations and G gene truncation reduces neurovirulence and enhances immunogenicity in mice. *J Virol* 82:207–219. <https://doi.org/10.1128/JVI.01515-07>.
 15. Mire CE, Matassov D, Geisbert JB, Latham TE, Agans KN, Xu R, Ota-Setlik A, Egan MA, Fenton KA, Clarke DK, Eldridge JH, Geisbert TW. 2015. Single-dose attenuated Vesiculovax vaccines protect primates against Ebola Makona virus. *Nature* 520:688–691. <https://doi.org/10.1038/nature14428>.
 16. Clarke DK, Nasar F, Chong S, Johnson JE, Coleman JW, Lee M, Witko SE, Kotash CS, Abdullah R, Megati S, Luckay A, Nowak B, Lackner A, Price RE, Little P, Kalyan N, Randolph V, Javadian A, Zamb TJ, Parks CL, Egan MA, Eldridge J, Hendry M, Udem SA. 2014. Neurovirulence and immunogenicity of attenuated recombinant vesicular stomatitis viruses in nonhuman primates. *J Virol* 88:6690–6701. <https://doi.org/10.1128/JVI.03441-13>.
 17. Matassov D, Marzi A, Latham T, Xu R, Ota-Setlik A, Feldmann F, Geisbert JB, Mire CE, Hamm S, Nowak B, Egan MA, Geisbert TW, Eldridge JH, Feldmann H, Clarke DK. 2015. Vaccination with a highly attenuated recombinant vesicular stomatitis virus vector protects against challenge with a lethal dose of Ebola virus. *J Infect Dis* 212:5443–5451. <https://doi.org/10.1093/infdis/jiv316>.
 18. Elizaga ML, Li SS, Kochar NK, Wilson GJ, Allen MA, Tieu HVN, Frank I, Sobieszczyk ME, Cohen KW, Sanchez B, Latham TE, Clarke DK, Egan MA, Eldridge JH, Hannaman D, Xu R, Ota-Setlik A, McElrath MJ, Hay CM, NIAID HIV Vaccine Trials Network 087 Study Team. 2018. Safety and tolerability of HIV-1 multiantigen pDNA vaccine given with IL-12 plasmid DNA via electroporation, boosted with a recombinant vesicular stomatitis virus HIV Gag vaccine in healthy volunteers in a randomized, controlled clinical trial. *PLoS One* 13:e0202753. <https://doi.org/10.1371/journal.pone.0202753>.
 19. Li SS, Kochar NK, Elizaga M, Hay CM, Wilson GJ, Cohen KW, De Rosa SC, Xu R, Ota-Setlik A, Morris D, Finak G, Allen M, Tieu HV, Frank I, Sobieszczyk ME, Hannaman D, Gottardo R, Gilbert PB, Tomaras GD, Corey L, Clarke DK, Egan MA, Eldridge JH, McElrath MJ, Frahm N, NIAID HIV Vaccine Trials Network. 2017. DNA priming increases frequency of T-cell responses to a vesicular stomatitis virus HIV vaccine with specific enhancement of CD8⁺ T-cell responses by interleukin-12 plasmid DNA. *Clin Vaccine Immunol* 24:e00263-17. <https://doi.org/10.1126/CI.00263-17>.
 20. Yang D, Liu L, Zhu D, Peng H, Su L, Fu Y, Zhang L. 2014. A mouse model for HBV immunotolerance and immunotherapy. *Cell Mol Immunol* 11:71–78. <https://doi.org/10.1038/cmi.2013.43>.
 21. Churchill GA, Gatti DM, Munger SC, Svenson KL. 2012. The Diversity Outbred mouse population. *Mamm Genome* 23:713–718. <https://doi.org/10.1007/s00335-012-9414-2>.
 22. Yang PL, Althage A, Chung J, Chisari FV. 2002. Hydrodynamic injection of viral DNA: a mouse model of acute hepatitis B virus infection. *Proc Natl Acad Sci U S A* 99:13825–13830. <https://doi.org/10.1073/pnas.202398599>.
 23. Dion S, Bourguine M, Godon O, Levillayer F, Michel ML. 2013. Adeno-associated virus-mediated gene transfer leads to persistent hepatitis B virus replication in mice expressing HLA-A2 and HLA-DR1 molecules. *J Virol* 87:5554–5563. <https://doi.org/10.1128/JVI.03134-12>.
 24. Huang LR, Wu HL, Chen PJ, Chen DS. 2006. An immunocompetent mouse model for the tolerance of human chronic hepatitis B virus infection. *Proc Natl Acad Sci U S A* 103:17862–17867. <https://doi.org/10.1073/pnas.0608578103>.
 25. Guidotti LG, Ishikawa T, Hobbs MV, Matzke B, Schreiber R, Chisari FV. 1996. Intracellular inactivation of the hepatitis B virus by cytotoxic T lymphocytes. *Immunity* 4:25–36. [https://doi.org/10.1016/S1074-7613\(00\)80295-2](https://doi.org/10.1016/S1074-7613(00)80295-2).
 26. Thimme R, Wieland S, Steiger C, Ghayeb J, Reimann KA, Purcell RH, Chisari FV. 2003. CD8⁺ T cells mediate viral clearance and disease pathogenesis during acute hepatitis B virus infection. *J Virol* 77:68–76. <https://doi.org/10.1128/JVI.77.1.68-76.2003>.
 27. Maini MK, Schurich A. 2010. The molecular basis of the failed immune response in chronic HBV: therapeutic implications. *J Hepatol* 52:616–619. <https://doi.org/10.1016/j.jhep.2009.12.017>.
 28. Hui CK, Lie A, Au WY, Leung YH, Ma SY, Cheung WW, Zhang HY, Chim CS, Kwong YL, Liang R, Lau GK. 2005. A long-term follow-up study on hepatitis B surface antigen-positive patients undergoing allogeneic hematopoietic stem cell transplantation. *Blood* 106:464–469. <https://doi.org/10.1182/blood-2005-02-0698>.
 29. Kosinska AD, Zhang E, Johrden L, Liu J, Seiz PL, Zhang X, Ma Z, Kemper T, Fiedler M, Glebe D, Wildner O, Dittmer U, Lu M, Roggendorf M. 2013. Combination of DNA prime-adenovirus boost immunization with entecavir elicits sustained control of chronic hepatitis B in the woodchuck model. *PLoS Pathog* 9:e1003391. <https://doi.org/10.1371/journal.ppat.1003391>.
 30. Menne S, Maschke J, Tolle TK, Lu M, Roggendorf M. 1997. Characterization of T-cell response to woodchuck hepatitis virus core protein and protection of woodchucks from infection by immunization with peptides containing a T-cell epitope. *J Virol* 71:65–74.
 31. Zhang E, Kosinska AD, Ma Z, Dietze KK, Xu Y, Meng Z, Zhang X, Wang J, Wang B, Dittmer U, Roggendorf M, Yang D, Lu M. 2015. Woodchuck hepatitis virus core antigen-based DNA and protein vaccines induce qualitatively different immune responses that affect T cell recall responses and antiviral effects. *Virology* 475:56–65. <https://doi.org/10.1016/j.virol.2014.11.004>.
 32. Galen JE, Curtiss R, III. 2014. The delicate balance in genetically engineering live vaccines. *Vaccine* 32:4376–4385. <https://doi.org/10.1016/j.vaccine.2013.12.026>.
 33. Robert-Guroff M. 2007. Replicating and non-replicating viral vectors for vaccine development. *Curr Opin Biotechnol* 18:546–556. <https://doi.org/10.1016/j.copbio.2007.10.010>.
 34. Buchmann P, Dembek C, Kuklick L, Jager C, Tedjukusumo R, von Freyend MJ, Drebber U, Janowicz Z, Melber K, Protzer U. 2013. A novel therapeutic hepatitis B vaccine induces cellular and humoral immune responses and breaks tolerance in hepatitis B virus (HBV) transgenic mice. *Vaccine* 31:1197–1203. <https://doi.org/10.1016/j.vaccine.2012.12.074>.
 35. Sette AD, Oseroff C, Sidney J, Alexander J, Chesnut RW, Kakimi K, Guidotti LG, Chisari FV. 2001. Overcoming T cell tolerance to the hepatitis B virus surface antigen in hepatitis B virus-transgenic mice. *J Immunol* 166:1389–1397. <https://doi.org/10.4049/jimmunol.166.2.1389>.
 36. Li J, Ge J, Ren S, Zhou T, Sun Y, Sun H, Gu Y, Huang H, Xu Z, Chen X, Xu X, Zhuang X, Song C, Jia F, Xu A, Yin X, Du SX. 2015. Hepatitis B surface antigen (HBsAg) and core antigen (HBcAg) combine CpG oligodeoxynucleotides [sic] as a novel therapeutic vaccine for chronic hepatitis B infection. *Vaccine* 33:4247–4254. <https://doi.org/10.1016/j.vaccine.2015.03.079>.
 37. Backes S, Jager C, Dembek CJ, Kosinska AD, Bauer T, Stephan AS, Dislers A, Mutwiri G, Busch DH, Babiuk LA, Gasteiger G, Protzer U. 2016. Protein-prime/modified vaccinia virus Ankara vector-boost vaccination overcomes tolerance in high-antigenemic HBV-transgenic mice. *Vaccine* 34:923–932. <https://doi.org/10.1016/j.vaccine.2015.12.060>.
 38. Martin P, Dubois C, Jacquier E, Dion S, Mancini-Bourguine M, Godon O, Kratzer R, Lelu-Santolaria K, Evlachev A, Meritet J-F, Schlesinger Y, Villeval D, Strub J-M, Van Dorsselaer A, Marchand J-B, Geist M, Brandely R, Findeli A, Boukheba H, Menguy T, Silvestre N, Michel M-L, Inchauspé G. 2015. TG1050, an immunotherapeutic to treat chronic hepatitis B, induces robust T cells and exerts an antiviral effect in HBV-persistent mice. *Gut* 64:1961–1971. <https://doi.org/10.1136/gutjnl-2014-308041>.
 39. Zhu D, Liu L, Yang D, Fu S, Bian Y, Sun Z, He J, Su L, Zhang L, Peng H, Fu YX. 2016. Clearing persistent extracellular antigen of hepatitis B virus: an immunomodulatory strategy to reverse tolerance for an effective therapeutic vaccination. *J Immunol* 196:3079–3087. <https://doi.org/10.4049/jimmunol.1502061>.

40. Bian Y, Zhang Z, Sun Z, Zhao J, Zhu D, Wang Y, Fu S, Guo J, Liu L, Su L, Wang FS, Fu YX, Peng H. 2017. Vaccines targeting preS1 domain overcome immune tolerance in hepatitis B virus carrier mice. *Hepatology* 66:1067–1082. <https://doi.org/10.1002/hep.29239>.
41. Zhao W, Zhou X, Zhao G, Lin Q, Wang X, Yu X, Wang B. 2017. Enrichment of Ly6C(hi) monocytes by multiple GM-CSF injections with HBV vaccine contributes to viral clearance in a HBV mouse model. *Hum Vaccin Immunother* 13:2872–2882. <https://doi.org/10.1080/21645515.2017.1344797>.
42. Kratzer R, Sansas B, Lelu K, Evlachev A, Schmitt D, Silvestre N, Inchauspe G, Martin P. 2018. A meta-analysis of the antiviral activity of the HBV-specific immunotherapeutic TG1050 confirms its value over a wide range of HBsAg levels in a persistent HBV pre-clinical model. *Hum Vaccin Immunother* 14:1417–1422. <https://doi.org/10.1080/21645515.2018.1433970>.
43. Laidlaw BJ, Craft JE, Kaech SM. 2016. The multifaceted role of CD4(+) T cells in CD8(+) T cell memory. *Nat Rev Immunol* 16:102–111. <https://doi.org/10.1038/nri.2015.10>.
44. Nakanishi Y, Lu B, Gerard C, Iwasaki A. 2009. CD8(+) T lymphocyte mobilization to virus-infected tissue requires CD4(+) T-cell help. *Nature* 462:510–513. <https://doi.org/10.1038/nature08511>.
45. Provine NM, Larocca RA, Aid M, Penalzoza-MacMaster P, Badamchi-Zadeh A, Borducchi EN, Yates KB, Abbink P, Kirilova M, Ng'ang'a D, Bramson J, Haining WN, Barouch DH. 2016. Immediate dysfunction of vaccine-elicited CD8+ T cells primed in the absence of CD4+ T cells. *J Immunol* 197:1809–1822. <https://doi.org/10.4049/jimmunol.1600591>.
46. Crouse J, Xu HC, Lang PA, Oxenius A. 2015. NK cells regulating T cell responses: mechanisms and outcome. *Trends Immunol* 36:49–58. <https://doi.org/10.1016/j.it.2014.11.001>.
47. Peppia D, Gill US, Reynolds G, Easom NJ, Pallett LJ, Schurich A, Micco L, Nebbia G, Singh HD, Adams DH, Kennedy PT, Maini MK. 2013. Up-regulation of a death receptor renders antiviral T cells susceptible to NK cell-mediated deletion. *J Exp Med* 210:99–114. <https://doi.org/10.1084/jem.20121172>.
48. Lucifora J, Salvetti A, Marniquet X, Maily L, Testoni B, Fusil F, Inchauspe A, Michelet M, Michel ML, Levrero M, Cortez P, Baumert TF, Cosset FL, Chailier C, Zoulim F, Duranton D. 2017. Detection of the hepatitis B virus (HBV) covalently-closed-circular DNA (cccDNA) in mice transduced with a recombinant AAV-HBV vector. *Antiviral Res* 145:14–19. <https://doi.org/10.1016/j.antiviral.2017.07.006>.
49. Guidotti LG, Matzke B, Schaller H, Chisari FV. 1995. High-level hepatitis B virus replication in transgenic mice. *J Virol* 69:6158–6169.
50. Ramsburg E, Publicover J, Buonocore L, Poholek A, Robek M, Palin A, Rose JK. 2005. A vesicular stomatitis virus recombinant expressing granulocyte-macrophage colony-stimulating factor induces enhanced T-cell responses and is highly attenuated for replication in animals. *J Virol* 79:15043–15053. <https://doi.org/10.1128/JVI.79.24.15043-15053.2005>.
51. Reynolds TD, Buonocore L, Rose NF, Rose JK, Robek MD. 2015. Virus-like vesicle-based therapeutic vaccine vectors for chronic hepatitis B virus infection. *J Virol* 89:10407–10415. <https://doi.org/10.1128/JVI.01184-15>.
52. Reynolds TD, Moshkani S, Robek MD. 2017. An ELISPOT-based assay to measure HBV-specific CD8+ T cell response in immunocompetent mice, p 237–248. *In* Guo H, Cuconati A (ed), *Methods in molecular biology: hepatitis B virus methods and protocols*. Humana Press, New York, NY.
53. Keasler VV, Hodgson AJ, Madden CR, Slagle BL. 2007. Enhancement of hepatitis B virus replication by the regulatory X protein in vitro and in vivo. *J Virol* 81:2656–2662. <https://doi.org/10.1128/JVI.02020-06>.
54. Garson JA, Grant PR, Ayliffe U, Ferns RB, Tedder RS. 2005. Real-time PCR quantitation of hepatitis B virus DNA using automated sample preparation and murine cytomegalovirus internal control. *J Virol Methods* 126: 207–213. <https://doi.org/10.1016/j.jviromet.2005.03.001>.